Ultra-thin L10-FePt for perpendicular anisotropy L10-FePt/Ag/[Co/Pd]30 pseudo spin valves

Pin Ho, Guchang Han, Kaihua He, Gan Moog Chow, and Jing-Sheng Chen

Citation: Journal of Applied Physics **115**, 17C102 (2014); doi: 10.1063/1.4853175
View online: http://dx.doi.org/10.1063/1.4853175
View Table of Contents: http://scitation.aip.org/content/aip/journal/jap/115/17?ver=pdfcov
Published by the AIP Publishing

Ultra-thin $L1_0$-FePt for perpendicular anisotropy $L1_0$-FePt/Ag/$[Co/Pd]_{30}$ pseudo spin valves

Pin Ho,[1] Guchang Han,[2] Kaihua He,[3] Gan Moog Chow,[1] and Jing-Sheng Chen[1,a)]
[1]*Department of Materials Science and Engineering, National University of Singapore, Singapore 117576*
[2]*Data Storage Institute, Agency of Science, Technology and Research (A*STAR), Singapore 117608*
[3]*School of Mathematics and Physics, China University of Geosciences, Wuhan 430074, China*

(Presented 5 November 2013; received 3 September 2013; accepted 3 October 2013; published online 6 January 2014)

Perpendicular anisotropy $L1_0$-FePt/Ag/$[Co/Pd]_{30}$ pseudo spin valves (PSVs) with ultra-thin $L1_0$-FePt alloy free layer possessing high anisotropy and thermal stability have been fabricated and studied. The thickness of the $L1_0$-FePt layer was varied between 2 and 4 nm. The PSV became increasingly decoupled with reduced $L1_0$-FePt thickness due to the larger difference between the coercivity of the $L1_0$-FePt and $[Co/Pd]_{30}$ films. The PSV with an ultra-thin $L1_0$-FePt free layer of 2 nm displayed a high K_u of 2.21×10^7 ergs/cm^3, high thermal stability of 84 and a largest giant magnetoresistance of 0.54%. © *2014 AIP Publishing LLC*. [http://dx.doi.org/10.1063/1.4853175]

Spin valves (SVs) and magnetic tunnel junctions (MTJs) with perpendicular magnetic anisotropy (PMA) are favourable for spintronics applications such as the spin transfer torque magnetic random access memory (STT-MRAM) as they promise an improvement in areal density, while maintaining thermal stability.[1,2] Materials such as $L1_0$-FePt are suitable candidates for the magnetic layers in the SVs and MTJs due to their high PMA. An ultra-thin free layer is desirable for spin transfer torque switching (STTS) as a reduction in the free layer volume brings about a reduction in the STTS critical current. At the same time, the ultra-thin free layer is required to possess a PMA high enough to ensure the non-volatility of the STT-MRAM.

Earlier, Yakushiji *et al*. demonstrated STTS in ultra-thin FePt, with thickness in the range of 1.02 to 2.04 nm, for the PMA $L1_0$-FePt based SV.[3] The ultra-thin $L1_0$-FePt was fabricated using the molecular beam epitaxial deposition of alternating $[Fe/Pt]_n$ multilayers. However, the use of the $[Fe/Pt]_n$ multilayer structure gives less stable magnetic properties which tend to fluctuate due to the interdiffusion of the Fe/Pt alternating layers.[4] An ultra-thin FePt alloy film will thus have an edge over the multilayer structures in this aspect but this has yet to be demonstrated. Earlier reports of $L1_0$-FePt SV structures showed free $L1_0$-FePt alloy films with thickness in the range of 4 to 20 nm.[5–9] The fabrication and study of ultra-thin, continuous $L1_0$-FePt alloy films for the free layer is crucial for future applications in the area of PMA $L1_0$-FePt based STT-MRAM. In this paper, we demonstrate a series of pseudo spin valve (PSV) structures which consists of an ultra-thin $L1_0$-FePt alloy layer with thickness between 2 and 4 nm. The structural, crystallographic, magnetic, and spin transport properties of the PSVs with varying thickness of the ultra-thin $L1_0$-FePt alloy film will be studied in detail.

Samples with the structure MgO substrate/Fe (1 nm)/Pd (20 nm)/Pt (4 nm)/Fe (1 nm)/$L1_0$-$Fe_{55}Pt_{45}$ (x nm)/Ag (5 nm), with x varied between 1 and 4 nm, were fabricated to investigate the properties of a single ultra-thin $L1_0$-FePt alloy layer. In addition, PSVs with the structure Fe (1 nm)/Pd (20 nm)/Pt (4 nm)/Fe (1 nm)/$L1_0$-$Fe_{55}Pt_{45}$ (y nm)/Ag (5 nm)/ [Co (0.3 nm)/Pd (0.8 nm)]$_{30}$/Pt (3 nm) were also fabricated on the single crystal (001)-textured MgO substrates, with y varied between 2 and 4 nm. The nominal thickness was obtained by calibrating the sputtering parameters with the reference sample. The samples were prepared using the magnetron sputtering system with a base pressure better than 8×10^{-7} Torr. In all of the samples, the Fe/Pd/Pt underlayers were deposited at 150 °C, while the Fe/$L1_0$-FePt layers at 380 °C. The Ag spacer layer and $[Co/Pd]_{30}$ layers were subsequently deposited at room temperature to minimize interlayer diffusion within the PSVs, in particular at the interfaces of the ferromagnets and spacer. Crystallographic structures were studied using X-ray diffraction (XRD) with Cu K_α radiation. High resolution transmission electron microscopy (HRTEM) was used for the microstructure analysis. Root mean square surface roughness was obtained using the atomic force microscopy (AFM) technique. Magnetic properties were characterized by the vibrating sample magnetometer (VSM). Current-in-plane (CIP) resistance measurements were made using a four point probe in the presence of a perpendicular-to-plane field. First principles calculations of the band structures were performed using the Vienna *ab initio* simulation package (VASP).[10]

TABLE I. A summary of the magnetic properties of the ultra-thin $L1_0$-FePt with thickness of 1, 2, 3, and 4 nm. TSF is defined by K_uV/k_BT, where K_u is the magnetocrystalline anisotropy constant, V is the volume of the free layer bit (assuming a device diameter of 10 nm), k_B is Boltzmann constant, and T is temperature.

$L1_0$-FePt thickness (nm)	M_s (emu/cm^3)	K_u ($\times 10^7$ ergs/cm^3)	H_c (kOe)	S^*	TSF
1	675	2.06	1.34	0.51	39
2	614	2.21	1.43	0.81	84
3	532	2.50	1.67	0.89	142
4	611	2.89	1.92	0.87	219

a)Author to whom correspondence should be addressed. Electronic mail: msecj@nus.edu.sg

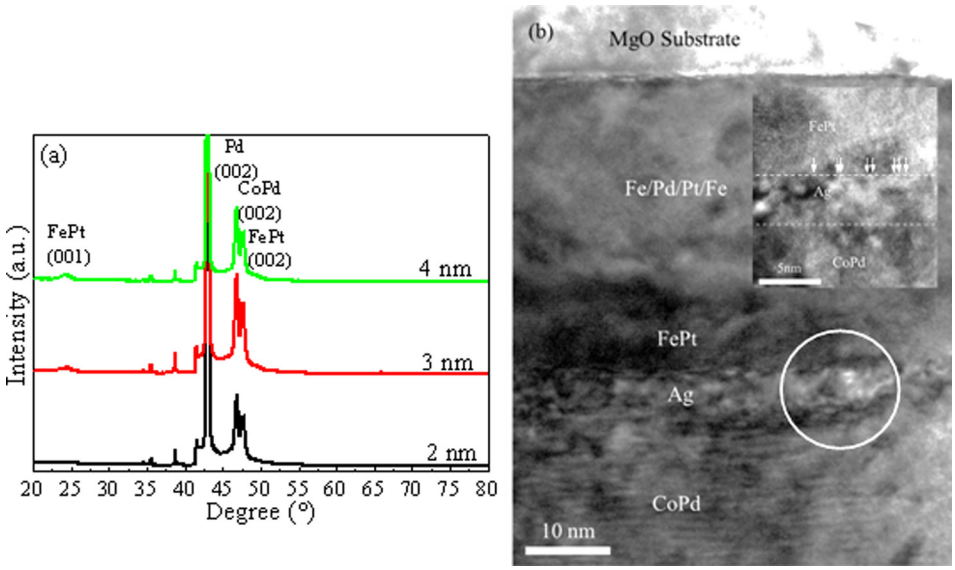

FIG. 1. (a) XRD spectrum of the PSVs with $L1_0$-FePt thickness of 2, 3, and 4 nm. The unlabelled sharp peaks are inherent of the MgO substrate. (b) Cross-sectional HRTEM image of the MgO substrate/Fe/Pd/Pt/Fe/$L1_0$-FePt/Ag/$[Co/Pd]_{30}$ PSV with $L1_0$-FePt thickness of 4 nm. Inset indicates the magnified cross section of the circled region. Dashed lines in the inset represent the FePt/Ag and Ag/CoPd interfaces.

Table I shows the magnetic properties of the ultra-thin $L1_0$-FePt with thickness varied from 1 to 4 nm. With increasing $L1_0$-FePt thickness, the PMA and thermal stability factor (TSF), K_uV/k_BT, of the ultra-thin $L1_0$-FePt layer increased. The thermal stability of the bit is critical for the maintenance of the non-volatility of the STT-MRAM, especially since the STT effect dominates only at small dimensions of less than 100 nm. A 10-year thermal stability criterion of greater than 60 is typically required. Assuming the scalability of the PSV to a diameter of 10 nm, these nanopillars with ultra-thin $L1_0$-FePt thickness of 2 to 4 nm possessed a TSF which surpassed the thermal stability criterion [Table I]. For the 1 nm $L1_0$-FePt, the squareness (S^*) and TSF were low and hence only the properties of the PSVs with $L1_0$-FePt thickness of 2 to 4 nm would be further explored in this paper. Fig. 1(a) shows the XRD spectrum of the PSVs with varying $L1_0$-FePt thickness. In all the PSVs, a (002) texture was formed for the Pd bottom electrode. This served to promote the subsequent $L1_0$ ordering in the FePt, evident from the superlattice (001) and fundamental (002) $L1_0$-FePt peaks. The (001) and (002) FePt peaks became more prominent with increasing $L1_0$-FePt thickness due to a stronger signal from a thicker $L1_0$-FePt. (002) textured perpendicular anisotropy $[Co/Pd]_{30}$ multilayer was also formed, induced by the growth of (001) $L1_0$-FePt and (002) Ag spacer [Fig. 1(a)]. Cross-sectional HRTEM of the PSV with $L1_0$-FePt thickness of 4 nm [Fig. 1(b) and inset] shows a crystalline growth of the (001)

TABLE II. A summary of the properties of the PSVs with ultra-thin $L1_0$-FePt thickness of 2, 3, and 4 nm. R_{rms} is the root mean square roughness of the Ag interface. H_{cfree} and H_{chard} are the coercivity of the free $L1_0$-FePt and hard $[Co/Pd]_{30}$ layers, respectively. Resistance and GMR of the PSVs with different $L1_0$-FePt thickness were measured. The GMR values do not include the background MR contribution.

$L1_0$-FePt thickness (nm)	R_{rms} (nm)	H_{cfree} (kOe)	H_{chard} (kOe)	Resistance (Ω)	GMR (%)
2	3.3	1.10	2.62	1.24	0.54
3	2.5	1.43	2.70	1.20	0.40
4	1.8	1.58	1.58	1.38	…

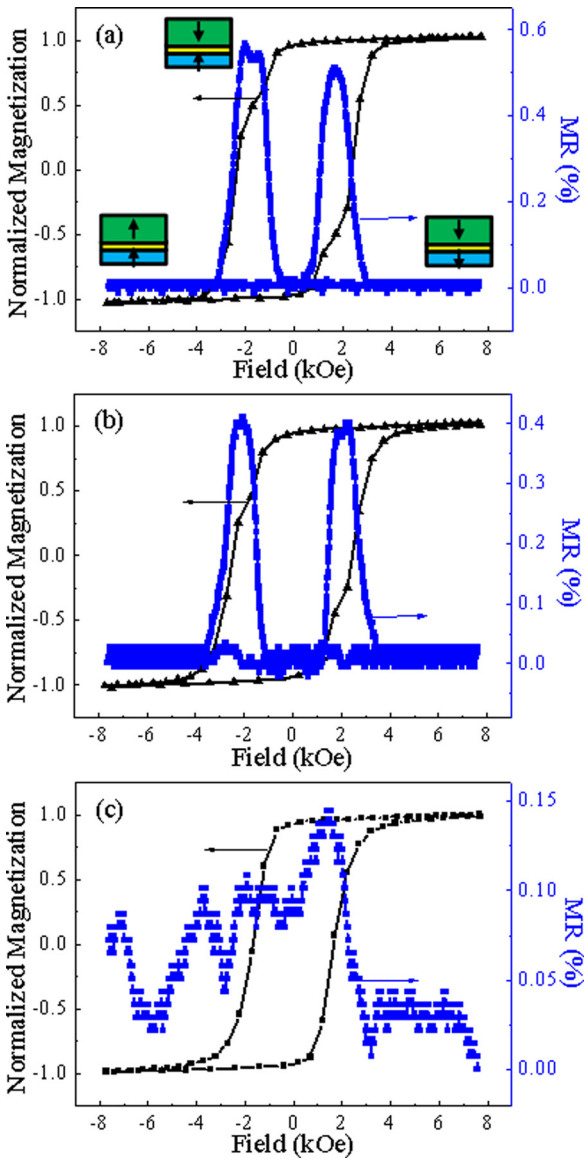

FIG. 2. Out-of-plane magnetization curves and MR curves measured at room temperature for PSVs with $L1_0$-FePt thickness of (a) 2, (b) 3, and (c) 4 nm. MR curves in (a) and (b) have been corrected to reflect the actual GMR by subtracting the slope of the background MR contribution.

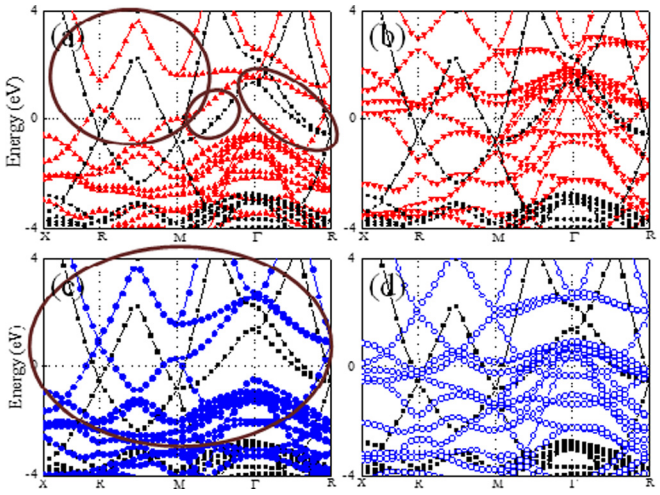

FIG. 3. The energy bands for the Ag (■) and (a) spin up FePt (▲), (b) spin down FePt (▼), (c) spin up Co (●), and (d) spin down Co (○). Better band match is evident around the Fermi energy of Ag with spin up FePt band and Ag with spin up Co band structures.

$L1_0$-FePt, (002) Ag spacer, and (002) $[Co/Pd]_{30}$ multilayer. The white arrows [Fig. 1(b) inset] highlight regions of mismatch at the $L1_0$-FePt/Ag interface which possibly arose due to the large lattice difference of 7.1% between FePt and Ag.

Table II summarizes the magnetic properties of the $L1_0$-FePt and $[Co/Pd]_{30}$ layers in the PSVs. With increasing $L1_0$-FePt thickness, the anisotropy and coercivity of the $L1_0$-FePt increased. This was attributed to the improvement in the $L1_0$ ordering due to the increased volume fraction of the fct $L1_0$-FePt formed with a thicker $L1_0$-FePt. The absence of independent reversal in the PSV with $L1_0$-FePt film thickness of 4 nm was attributed to the similarity in coercivity between the $L1_0$-FePt and $[Co/Pd]_{30}$ layers [Fig. 2(c)]. With the $L1_0$-FePt film thickness reduced, decoupling between the $L1_0$-FePt and $[Co/Pd]_{30}$ layers was observed [Figs. 2(a) and 2(b)]. The softer $L1_0$-FePt and harder $[Co/Pd]_{30}$ acted as the free and fixed layer, respectively.

When the $L1_0$-FePt layer thickness was 4 nm, the absence of a distinct difference between the coercivities of the $L1_0$-FePt and $[Co/Pd]_{30}$ layers resulted in a persistently parallel configuration of the ferromagnetic (FM) layers. As such, only a background magnetoresistance (MR) which arose from the finite temperature effect was observed [Fig. 2(c)].[11] The background MR contribution possessed a largest value of 0.15% in the absence of an applied field. This MR gradually decreased with a larger applied field which eliminated the *s-d* electrons spin flipping disorder. With reduced $L1_0$-FePt thickness, a giant magnetoresistance (GMR) was produced due to the formation of the parallel and anti-parallel configurations of the $L1_0$-FePt and $[Co/Pd]_{30}$ layers with applied field, which gave rise to the low and high resistance states, respectively [Fig. 2(a) inset]. Fig. 3 shows that near the Fermi energy level of 0 eV, both the band structures of FePt and Co spin up electrons displayed better band compatibility with Ag, in terms of more similar energy and slope, compared to that of the FePt and Co spin down electrons.[12] As such, majority spin up electrons would be scattered less extensively compared to the spin down electrons at the FePt/Ag and Ag/Co interfaces, contributing to a larger transmission of majority spin up electrons across the interfaces. This reinforces that the GMR observed was attributed to the differential scattering of the spin up and spin down conduction electrons at the $L1_0$-FePt/Ag and Ag/Co interfaces of the PSVs. In the parallel configuration, the majority spin up electrons passed through relatively easily, giving a low resistance state. In the anti-parallel configuration, the electrons in both channels were reflected at either one of the interfaces, producing a higher resistance state. In addition, a positive GMR was observed since the surface and bulk spin asymmetries of the $L1_0$-FePt and $[Co/Pd]_{30}$ magnetic films possessed positive values, indicating that the majority spin up electrons were less scattered within the layers and at the interfaces.[13]

With a reduction in the $L1_0$-FePt layer thickness to 2 nm, the GMR increased to a highest value of 0.54% (Table II). This was attributed to a more decoupled PSV where the $L1_0$-FePt and $[Co/Pd]_{30}$ layers possessed a more distinct difference in their coercivity. A better decoupled PSV suggests a smaller extent of mutual influence between the spins of both FM layers, thereby allowing a greater proportion of spins to possess opposite magnetization. Another contribution could also be due to the smaller number of heavy Pt scattering centres present in the thinner FePt films, which reduced the extent of spin dependent scattering.[14]

This work was supported by Ministry of Education, Singapore, Tier 2 funding, MOE2012-T2-2-031.

[1]J. G. Zhu, Proc. IEEE **96**, 1786 (2008).
[2]R. Sbiaa, H. Meng, and S. N. Piramanayagam, Phys. Status Solidi (RRL) **5**, 413 (2011).
[3]K. Yakushiji, S. Yuasa, T. Nagahama, A. Fukushima, H. Kubota, T. Katayama, and K. Ando, Appl. Phys. Express **1**, 041302 (2008).
[4]C. S. E. J. Rantschler, S. S. Zhang, S. Khizroev, T. R. Lee, and D. Litvinov, J. Appl. Phys. **103**, 113910 (2008).
[5]T. Seki, S. Mitani, K. Yakushiji, and K. Takanashi, Appl. Phys. Lett. **89**, 172504 (2006).
[6]A. P. Mihai, J. P. Attané, L. Vila, C. Beigné, J. C. Pillet, and A. Marty, Appl. Phys. Lett. **94**, 122509 (2009).
[7]C. L. Zha, J. Persson, S. Bonetti, Y. Y. Fang, and J. Akerman, Appl. Phys. Lett. **94**, 163108 (2009).
[8]P. Ho, G. C. Han, R. F. L. Evans, R. W. Chantrell, G. M. Chow, and J. S. Chen, Appl. Phys. Lett. **98**, 132501 (2011).
[9]P. Ho, G. C. Han, K. H. He, G. M. Chow, and J. S. Chen, Appl. Phys. Lett. **99**, 252503 (2011).
[10]G. Kresse and J. Hafner, Phys. Rev. B **47**, 558 (1993); **49**, 14251 (1994).
[11]J. Yu, U. Rüdiger, A. D. Kent, R. F. C. Farrow, R. F. Marks, D. Weller, L. Folks, and S. S. P. Parkin, J. Appl. Phys. **87**, 6854 (2000).
[12]T. Ambrose and O. Mryasov, *Half-Metallic Alloys Fundamentals and Applications*, edited by I. Galanakis and P. H. Dederichs (Springer, Berlin, 2005), pp. 206–210.
[13]J. Barnas, A. Fert, M. Gmitra, I. Weymann, and V. K. Dugaev, Phys. Rev. B. **72**, 024426 (2005).
[14]A. D. Kent, Nature Mater. **9**, 699 (2010).